

# FLIGHT PERFORMANCE AND STABILITY OF SPACE LAUNCH SYSTEM CORE STAGE THRUST VECTOR CONTROL

John H. Wall\*, Colter W. Russell†, Jeb S. Orr‡, Abran Alaniz§, and Stephen G. Ryan¶

The Space Launch System (SLS) Core Stage (CS) Thrust Vector Control (TVC) system is comprised of eight mechanical feedback Shuttle heritage Type III TVC actuators and four RS-25 engines, each attached to a Shuttle heritage gimbal block/bearing. The Core Stage TVC shares vehicle control authority with the SLS 5-segment Solid Rocket Boosters (SRBs) during boost phase flight, and is the sole means of vehicle flight control during in exoatmospheric flight following SRB separation.

TVC responses during Green Run Hot Fire (GRHF) testing revealed that the TVC did not meet its performance specifications. Step and frequency responses exhibited unexpected departures from prior laboratory data and modeled behavior. Post-test analysis determined that the characteristics of the structure and gimbal friction are significantly influenced by the thrust-loaded conditions, and the command avionics exhibited a small but important gain nonlinearity. Using the available test data, the design team augmented the flight control TVC models to bound the observed results and include the additional fidelity needed for vehicle flight control analysis so as to build sufficient rationale for flight certification.

Prior to the Green Run tests, “simplex” linear models typically used for flight control analysis did not include gimbal friction and other nonlinearities owing to long-standing assumptions that these effects were negligible in the Shuttle Orbiter TVC system. Following the Green Run findings, simulation analysis of the flight dynamics in the time and frequency domain revealed the propensity for a flight control limit cycle oscillation (LCO) if friction and structural compliances fell near the edges of test-predicted bounds. While the “most probable” models did not predict an in-flight LCO, the SLS Program conservatively proceeded with a system-wide evaluation and ultimate acceptance of the possibility for a small-amplitude, low-frequency TVC LCO in flight. A final validation of the extensive test and modeling effort occurred when the first flight of SLS successfully demonstrated the fully integrated performance of the vehicle’s TVC system.

This paper is the final installment in a seven-paper series surveying the design, engineering, test validation, and flight performance of the Core Stage Thrust Vector Control system. In this paper, the development of flight rationale in light of the TVC responses observed in Green Run is discussed, along with a review of the flight telemetry illustrating the correlation of the preflight predictions with the observed performance.

---

\*SLS Flight Controls Lead, Mclaurin Aerospace (Jacobs ESSCA), Huntsville, AL

†Flight Systems Technical Staff, Mclaurin Aerospace (Jacobs ESSCA), Knoxville, TN

‡SLS Flight Dynamics and Control Technical Specialist, Mclaurin Aerospace (Jacobs ESSCA), Knoxville, TN

§Flight Systems Principal Staff, Mclaurin Aerospace (Jacobs ESSCA), Houston, TX

¶SLS Chief Engineer’s Office (MTS CPSS), Huntsville, AL

## 1 INTRODUCTION

The Space Launch System (SLS) thrust vector control system sought to minimize development cost and complexity by reusing hydraulic actuator hardware from the Space Shuttle Orbiter. Leveraging the "heritage" actuators but cognizant of their new application on an entirely redesigned SLS thrust structure, the NASA flight control discipline developed a comprehensive set of TVC requirements and performance specifications to ensure robust and stable vehicle flight control from liftoff through Main Engine Cut Off (MECO), the end of powered ascent flight.

The initial verification plan as developed by the core stage contractor relied solely on heritage linear ("simplex") models and did not explicitly link requirements verification to integrated system testing. The SLS flight control team, with the support of NASA engineering management, worked early in the program lifecycle to successfully baseline hot fire vectoring tests on the fully integrated core stage at the Green Run opportunity. Throughout the course of the Green Run test activities, the flight control discipline worked directly with TVC subsystem engineers and program stakeholders to develop and execute test objectives and data analysis to support model validation and reduce overall integration risk. Key ambient (non-firing) frequency response tests were added prior to hot fire, which proved essential in revealing the load stiffness in the non-thrusting environment and in demonstrating that friction was negligible in the unloaded gimbal configuration. In contrast, the hot fire tests showed that the loaded gimbal produced noticeable friction effects, which challenged the long-standing assumption that it was negligible during flight.<sup>1,2</sup> The hot fire vectoring test further revealed that the apparent load stiffness was significantly higher than in the ambient condition, which was later determined to be the result of the gimbal structural characteristics under load and the amplitude-dependent response characteristics of the actuator.<sup>1,7</sup> Following the Green Run test series, the flight control, TVC, and loads teams worked to assess the data for root cause of the observed test discrepancies. These insights were used to develop models for flight control analysis as well as models that would predict the response observed under test conditions.

The most significant observation during testing was that actuator step and frequency response specifications were not met in either the ambient or hot fire condition. After extensive analysis to determine that the dynamic response did not pose a risk to the Artemis I vehicle configuration's flight control stability and performance, flight rationale was developed to accept the deviation for the requirements for the first flight only. This approach allowed NASA to progress towards first flight with bounding model analysis, yet leave the opportunity for future changes for subsequent missions and vehicles. To build rationale for the first flight, the team worked to determine a set of bounding TVC models that captured the salient gimbal friction, load stiffness, and command avionics characteristics revealed at Green Run. The Artemis I flight bounding model analysis predicted a potential low frequency, small-amplitude flight control limit cycle. The Artemis I flight rationale was accepted after all stakeholders demonstrated that these small oscillations were not of significant concern. Due to the sharing of TVC control authority with the two 5-Segment Solid Rocket Boosters (SRBs) during the atmospheric boost phase, the limit cycle predictions were predicted to occur only following booster separation.

An extensive review of Space Shuttle flight data did not reveal any evidence of a limit cycle in flight, despite an identical engine, gimbal bearing, and similar structural characteristics. As such, the flight control team was not fully convinced that a Core Stage flight LCO on Artemis I was credible. Following the acceptance of flight rationale with bounding evaluations, the team significantly improved the fidelity of models with respect to the interaction of the structure and friction effects, in order to support flight rationale for the SLS program's planned manifest. A special analysis team

was formed including representatives from the core stage contractor, the RS-25 engine contractor, NASA TVC, NASA Loads and Dynamics, and NASA's Flight Control engineers. The results of this year-long investigation revealed that the apparent increase in the load stiffness between ambient and hot fire conditions could be explained by the change in load path for the thrust-loaded gimbal bearing, combined with amplitude-dependent nonlinearities in the response. After having identified a credible, physical mechanism for the observed behavior, the flight load characteristics could be assumed closer to those seen during Green Run hot fire. Advances in friction modeling of the gimbal joint extended the Dahl and LuGre models to account for the reduced effect of friction at small velocities, a counterintuitive behavior that is consistent with the presence of vibrational environment.<sup>2</sup> Unlike simple Coulomb models, which exhibit significant amplitude-dependent behavior for low-frequency command inputs, a modified LuGre model provides a mechanism to reduce static friction below that of dynamic friction in a way that is consistent with the observed response.

The NASA-developed coupled TVC-structure simulation model, Multiple Actuator Stage Vectoring (MASV), was used prior to Green Run to assess the interaction between TVC system and the vehicle structure "seen" by the actuator. MASV utilizes a modal representation of the vehicle's elastic dynamics including the core stage structure, engine gimbals, and engines, derived from detailed Finite Element Models (FEMs), and integrates these dynamics with linear models of all eight core stage actuators and their associated degrees of freedom.<sup>10</sup> MASV was updated after Green Run and helped confirm the load resonance (piston transfer function) responses seen between hot fire and ambient conditions. MASV confirmed, through analysis, a key Green Run test objective: that engine section local modes, despite their frequency density near the actuator bandwidth, do not adversely couple with the actuator position feedback servocontrol loop. MASV also demonstrated that while some dynamic coupling between the engines was present, it was not of enough significance to warrant explicit modeling for flight, nor was it responsible for the performance anomalies observed during Green Run.

A subsequent modeling effort attempted to develop the simplest possible representation that could reproduce the observed test response, having a single engine but two actuators kinematically coupled to multiple engine degrees of freedom. This multibody model, called TAOS (Two Actuator Operational Simulation), extended the linear "simplex" (planar) model of the TVC system. Most importantly, TAOS incorporates advanced friction models that impart forces on both halves of the gimbal joint, each represented as a stiffness matrix derived from a detailed gimbal FEM. The friction loads are calculated taking into account the geometry of the spherical bearing surface. This was later shown to be a key factor due to the fact that the Green Run vectoring test profiles, due to limited test time, commanded two engine axes simultaneously at different frequencies. While TAOS used a simplified backup structure model (similar to the simplex model), a spherical bearing, modified LuGre friction model was able to provide an excellent match to the Green Run characteristics in several respects. The inclusion of the out-of-plane gimbal DoF was shown to result in significantly different amplitude-dependent frequency response than that predicted by the planar simplex model with the same friction model, highlighting the importance of the gimbal joint's influence in the dynamic response.<sup>2</sup>

Review of telemetry from the highly successful Artemis I flight showed that the core stage commanded angles were within a tight range of nominal predictions and maintained high-performance control throughout the entirety of ascent flight. Evidence of small amplitude frequency content in the flight control response near the flight control gain crossover suggest that the effects of gimbal friction could have influenced the small amplitude behavior, as pre-flight models predicted. While

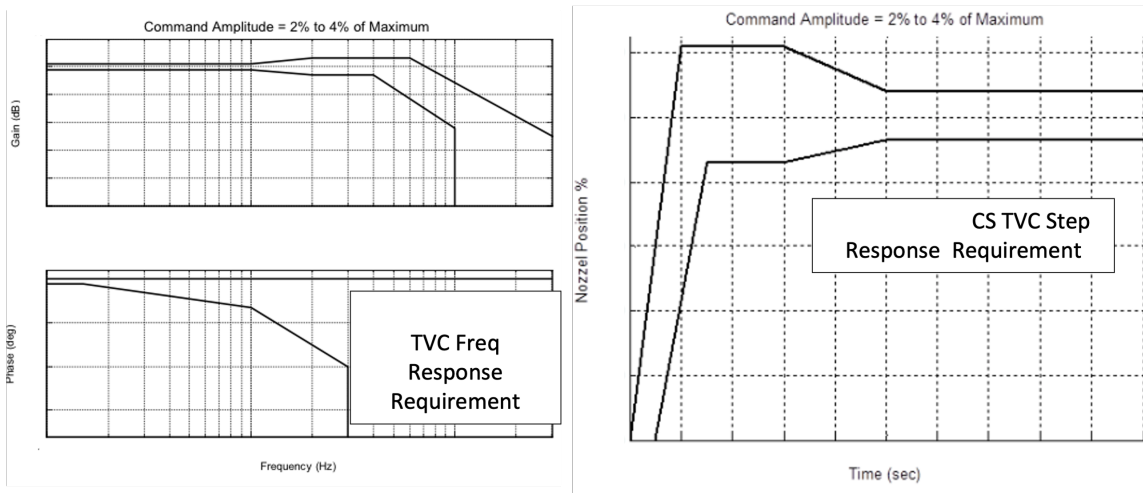


**Figure 1. Core Stage TVC Specifications**

the time responses do not show a clearly organized LCO as would be predicted by simulation, the in-flight gain and phase observations during Program Test Input (PTI) inputs show a characteristic suggesting that the modified LuGre friction modeling approach is appropriate.

## 2 TVC UPDATES FOLLOWING GREEN RUN FINDINGS

Following the Green Run test, both ambient and hot fire test data suggested that the TVC system did not meet the frequency and step response requirements shown in Figure 1.

As the original requirements were written to represent the response of the gimbal command to the engine angle in the flight condition, the data that provided a means to directly verify this requirement were engine angles derived from 16 dual-redundant linear string potentiometers or “string pots” mounted on the core stage heat shield. Due to constraints associated with placement of the sensors, the string pot measurements could not provide an absolute reference to determine the engine angles. For this reason and since Green Run is only an approximation of flight boundary conditions, complete verification of the subject requirements depended on having a test-validated model configured with flight parameters.

The observed discrepancies in the TVC response during the Green Run test series was dominated by three categories of phenomena: the characteristics of the structure and its influence on the apparent engine-structure load resonance, the presence and nature of gimbal friction, and a small nonlinearity in the TVC avionics command path. Utilizing a bounding approach, the effects of various candidate friction models, a range of assumed load stiffnesses, and the lowest command gain from the electronics were added to the linear simplex model. These models were used in the flight control analysis to support the bounding evaluations of the responses and build Artemis I flight rationale. Each of these phenomena are discussed in the sections that follow.

### 2.1 Friction

Hot fire testing revealed indications of gimbal friction in the frequency and step responses. Based on Shuttle and Saturn flight data and long-standing NASA MSFC flight control experience, the observable effects of friction in the Orbiter heritage gimbal bearing were previously presumed to be

inconsequential, owing to an assumed vibration dither effect.. While detailed TVC models have included friction effects within the TVC actuator mechanism,<sup>8</sup> models of gimbal friction were excluded in the simplified TVC models used for requirements verification prior to testing. The flight control team subsequently updated the simplex model to incorporate various gimbal friction models, including:

- Simple Coulomb friction, using Keene’s method<sup>4</sup> or Brouwer’s<sup>3</sup> method to ensure numerical stability and eliminate chatter.
- Dahl<sup>5</sup> friction, which includes a position dependent phenomena whereby the friction force acts like a spring for small displacements from a state of rest.
- LuGre<sup>6</sup> friction, which extends Dahl to include a velocity dependent effect for more accurate representation between the transition between static friction (also known as stiction) and dynamic friction.

The friction model parameters were tuned in an attempt to match the Green Run hot fire responses, as well as to correlate with historical Space Shuttle Main Propulsion Test Article (MPTA) testing. The Shuttle MPTA results provided key friction information not collected at Green Run including a pressure-based means of load measurement during multi-ramp commanding that provided an estimate of the Coulomb friction torque. The Shuttle MPTA data also provided some indication of amplitude dependent frequency response,<sup>8</sup> a key factor in determining the propensity for limit cycling in the control loop. A companion paper provides a description of the friction modeling approaches as well as advances to the LuGre model to modulate the stiction effect based on vibrational environments.<sup>2</sup>

## 2.2 Stiffness

The Green Run test series revealed a difference in the load stiffness between ambient and hot fire conditions via a change in the apparent load resonance frequency in the command to piston position transfer function.<sup>1</sup> The load resonance is a key parameter in the TVC models that represents the equivalent load path associated with all compliances outside of the actuator position control loop, i.e., the thrust structure, engine structure, gimbal, actuator case, and associated secondary structure. With knowledge of engine inertia  $J_n$  (including propellant), and the actuator moment arm  $R$ , the load stiffness  $K_L$  can be determined the load resonance frequency  $\omega_L$ , using Equation 1 below. The engine rotational stiffness  $K_n$  (which represents propellant feedline loads and gravitational terms) also influences the load resonance frequency but is typically negligible compared with the structural effects.

$$\omega_L = \sqrt{\frac{K_L R^2 + K_n}{J_n}} \quad (1)$$

The load resonance frequency  $\omega_L$  can be directly observed as the characteristic notch frequency in the command to piston position transfer function derived from frequency response testing.<sup>11</sup> Figure 2 shows the gain response from ambient (left) and hot fire (right) test conditions (circles) along with model responses (lines) after fitting  $K_L$  to the test data. As will be shown in Section 3, a more compliant thrust structure exhibits the highest risk for flight control loop limit cycle when combined

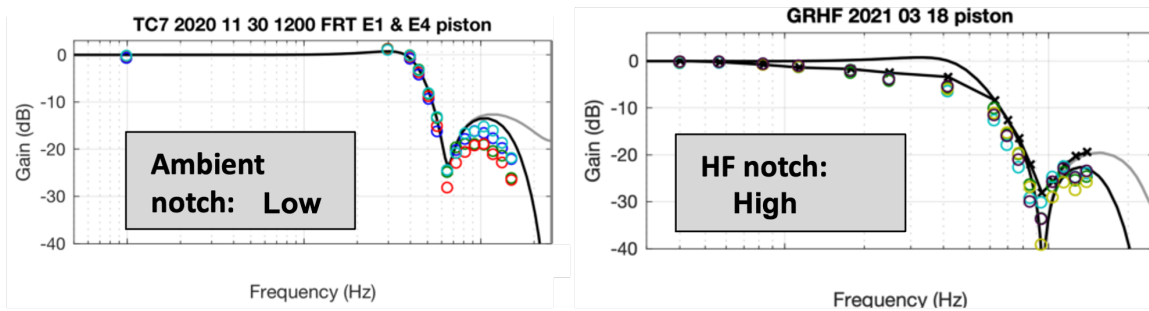


**Figure 2. TVC Command to Piston Position Frequency Response in Ambient and Hot Fire Conditions**

with gimbal friction, since a softer structure exaggerates the degradation in gain and phase response in the engine angle command path. While the analysis team eventually determined that the gimbal characteristics under load and small amplitude nonlinearities were primary factors affecting the observed load resonance frequency, the bounding models for flight rationale assumed the lowest (most conservative) of the two values, as anchored to the ambient test.

### 2.3 Avionics

A DC gain offset was observed in the sensed current telemetry in the lab and Green Run responses showing approximately -1 dB of gain reduction in the step and frequency response data. Following discussions with the TVC Actuator Controller (TAC) vendor, this was found to be the result of crossover distortion in TAC servo amplifier, a component redesigned for SLS to mimic the function of the Space Shuttle Ascent Thrust Vector Controller (ATVC) hardware. The TAC vendor described the input-output relationship with a curve representing the error as a function of command input. The maximum error results in about 95% of the commanded value (-1.1 dB) and corresponds to the region in which most of the flight commanding would be expected to occur.

Using the Systems Integration Lab (SIL) environment at MSFC, a full hardware-in-the-loop simulation facility, the analytically-predicted gain errors were confirmed using representative TAC flight hardware. The main goal of the SIL verification activity was to determine the detailed behavior near the important low-amplitude region. It was also used to rule out any other frequency-dependent characteristics that might be present in the command electronics. The findings from this test validated the vendor-supplied analytical model and showed no unexpected frequency-dependent effects associated with the monitored actual servo current outputs.

However, the test also revealed some unexpected results. Figure 3 shows the low frequency multi-amplitude command results from the SIL test, monitoring the variety of signals from scripted “FCS” command, the MIL-STD-1553 bus command, the TAC command received, and then TAC sensed servo amplifier current and “blackboard” lab-monitored TVC servo currents (instrumented output of the TAC hardware). This data served to verify that the TAC sensed and instrumented current showed agreement at low frequency and followed the trend of the analytically-predicted curve (red line), including the valley-like effect. However, as amplitudes approached values lower than approximately 0.1 deg, the FSW commands placed on the bus (“bus cmd”) appeared to exhibit a scale factor nonlinearity as well, which also appeared on the TAC cmd. This gain effect, compounding with the servo amplifier gain, was determined to be the result of a truncation operation in the quantization of the commands in the vehicle-level software. This truncation effect is also the cause of

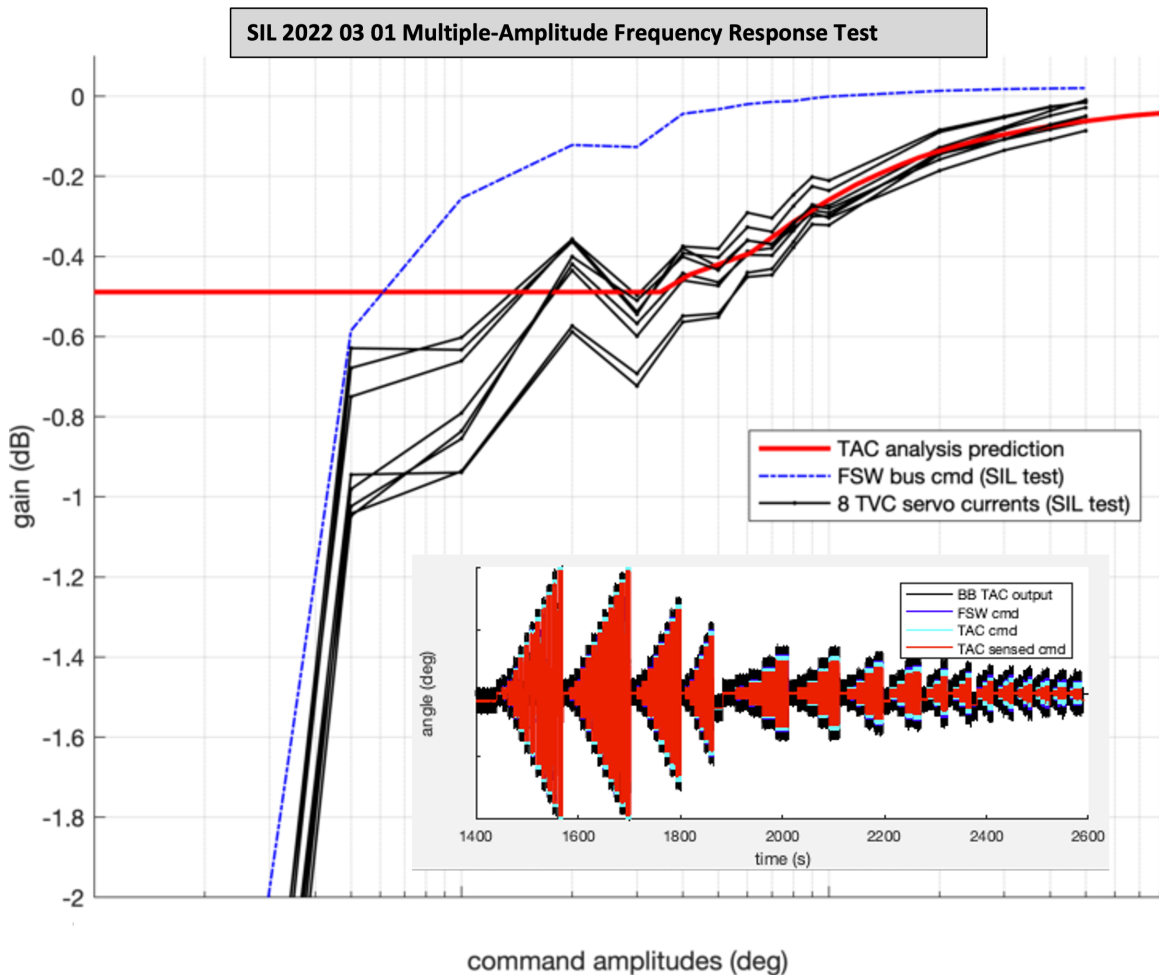


**Figure 3. SIL-Derived TAC Command Nonlinear Gain**

the precipitous drop off in the apparent gain for amplitudes below approximately 0.01 degree, given that the 12-bit FSW command resolution yields a least significant bit (LSB) of  $\sim 0.005$  deg (half the commanded value). The SLS Flight Software team subsequently planned to incorporate a rounding operation in future Block 1B mission builds to eliminate this effect. Likewise, the actuator vendor plans to update the servo amplifier electronics to include the necessary circuit elements to eliminate the nonlinearity and effectively eliminate the scale factor error.

These small-amplitude commands effect were considered to be at most responsible for a -1 dB decrease in flight control loop gain (for reasonable TVC motions above base quantization level) and such a gain was applied during the bounding model assessment. This gain level, in isolation, is not of great concern due to adequate low frequency gain margin in the flight control loop during Core Stage flight. However, this effect is retained for bounding model assessments due to its potential effect on the flight control limit cycle characteristics.

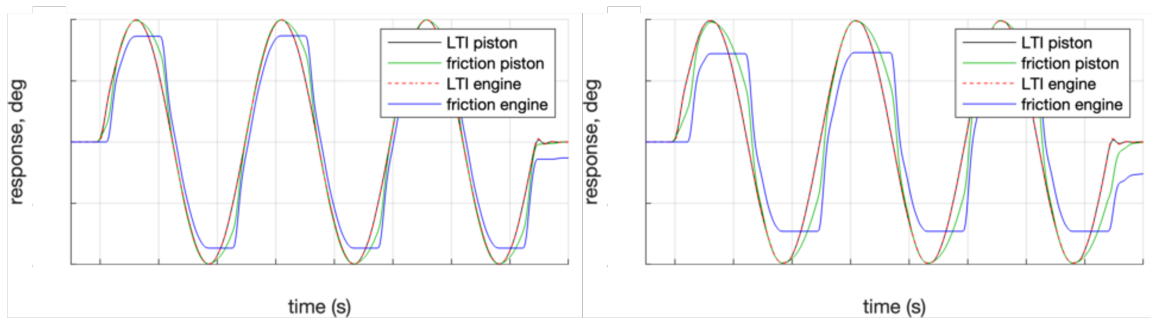


Figure 4. Example TVC Time Response with Simple Coulomb Friction in Gimbal

### 3 FLIGHT CONTROL RESPONSE WITH BOUNDING MODELS FOR FLIGHT RATIO-NALE

The two main concerns resulting from the presence of the gimbal friction and a reduced TVC load stiffness are in-flight limit cycle oscillation (LCO) and a reduction in the beneficial damping of high-frequency (6+ Hz) global vehicle structural modes provided by the core stage actuators. The following two sections describe the analysis that addresses each of these concerns.

#### 3.1 Illustration of How TVC Friction Produces Flight Control System LCO

Introduction of a gimbal friction model nonlinearity into the TVC actuator model will produce an amplitude-dependent response. Figure 4 compares the predicted response of engine and piston with gimbal friction to that of a purely linear time invariant model (“LTI”). A low frequency sinusoidal input is shown for an amplitude (left) and half that amplitude input (right). For a given amplitude of command input, friction will cause the output to lag that of the linear model and the output will fail to reach the full linear peak amplitude. Because only the piston position is controlled in the actuator feedback loop, and not the nozzle directly, the friction forces restrict the nozzle’s ability to fully deflect, being balanced against the deflection of the compliant structure. As command amplitude decreases, the elastic and inertial forces reduce proportionally, but the friction force is held constant. This results in in the appearance of further gain and phase degradation for smaller and smaller amplitudes, until at some amplitude the nozzle remains stationary while the structure deflects.

Using the friction-augmented simplex model, reconstructing the frequency response from command to piston and nozzle angle time histories quantifies the gain and phase degradation for a given command amplitude. Figure 5 shows the corresponding frequency-domain response for the same two amplitudes shown in the time response. The linear response curves are shown in solid lines and the simplex (labeled as Friction GR) responses augmented simple coulomb gimbal friction responses are shown with circle markers. The friction response for the higher command amplitude (left) decreases the DC gain of the nozzle but not the piston response, whose error is nulled by servo feedback. The phase effect of friction can be observed on both the piston and engine quantities. As expected, more substantial gain and phase variations are observed at higher frequencies. As the command amplitude is reduced (half amplitude shown in right figure), the same effects are observed to an exaggerated extent. Of particular importance is the DC gain and phase effect of the nozzle position. While the piston DC gain and phase are essentially unaffected, the nozzle position gain and phase is significantly degraded as the amplitude of the command is decreased. For the simple

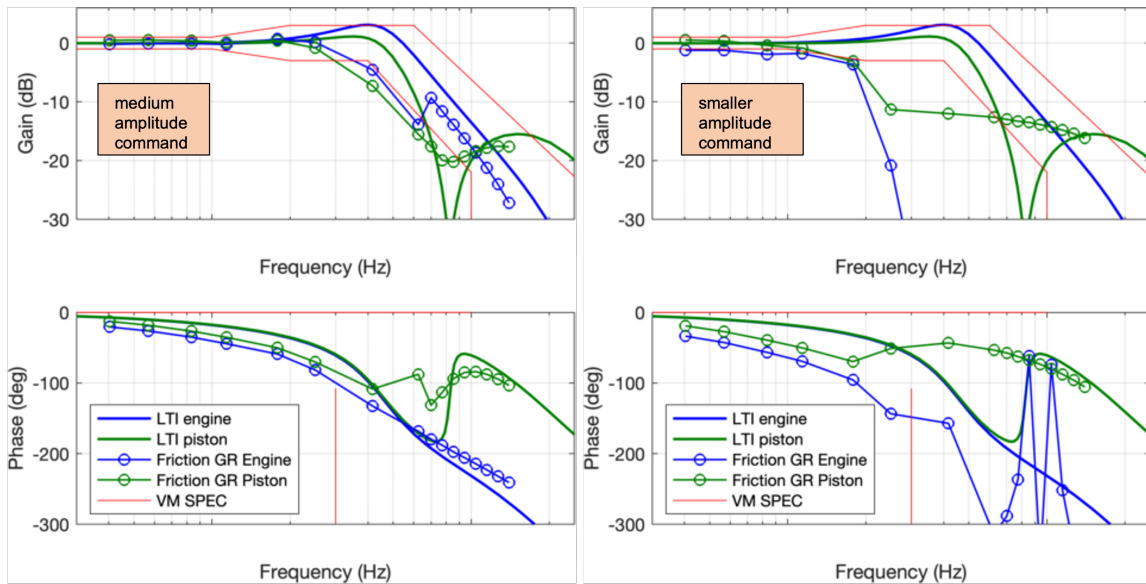


**Figure 5. Example TVC Frequency Response with Coulomb Friction**

friction model shown in this example, the lower amplitude gain plot (right) shows that the engine response fails to respond to any command beyond a frequency prior to its linear rolloff, despite piston movements. This is because the friction load fully inhibits gimbal movement and all the piston deflection is transferred into the structure. As such, a softer structure can exaggerate the effects of friction and the load stiffness is particularly important when evaluating the propensity for LCO.

Notionally representative Flight Control System (FCS) open-loop nominal responses are shown in the Nichols chart in Figure 6 with the vehicle loop gain and phase margins meeting the typical margins<sup>17</sup> at sufficiently high TVC command amplitudes. Since the TVC actuator is in the FCS forward path, a reduction in TVC gain or phase degrades flight control margins by the same amount. As determined by describing function analysis, the TVC command amplitude at which the friction-degraded response intersects the critical point indicates the predicted amplitude of a sustained in-flight limit cycle oscillation, or LCO.

### 3.2 Limit Cycle Predictions Using Bounding Models

The candidate friction models including Coulomb, Dahl, and LuGre were evaluated in the simplex model to determine the best fit to the observed Green Run test response. Due to limited test time during Core Stage hot fire, only a single set of amplitudes were exercised in test: 0.4 deg for low frequency commands (up to 7 Hz) and 0.8 deg for high frequency commands (up to 14 Hz). These limited data did not allow analysis to anchor the amplitude-dependent effects of the model fit. Furthermore, since the string pot derived engine responses did not provide an absolute reference for actual engine position, the DC gain response could not be determined from Green Run. Since the DC gain effect due to friction is almost completely isolated to the engine and not the piston response, the extent of friction degrading effects would not be fully observable at Green Run and thus a bounding model would be of paramount importance for predicting potential for LCO.

The Coulomb friction model, exhibited the most amplitude-dependent effects but did not compare well to the Green Run frequency responses. A modified form of LuGre exhibited the closest match

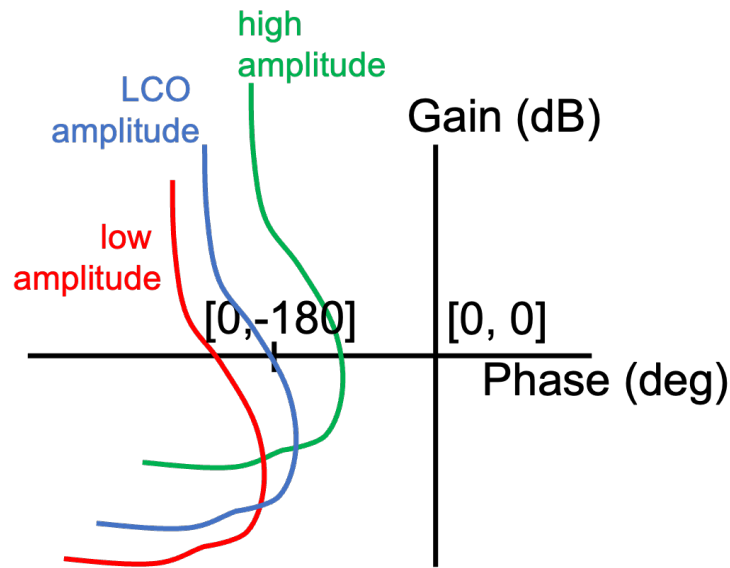


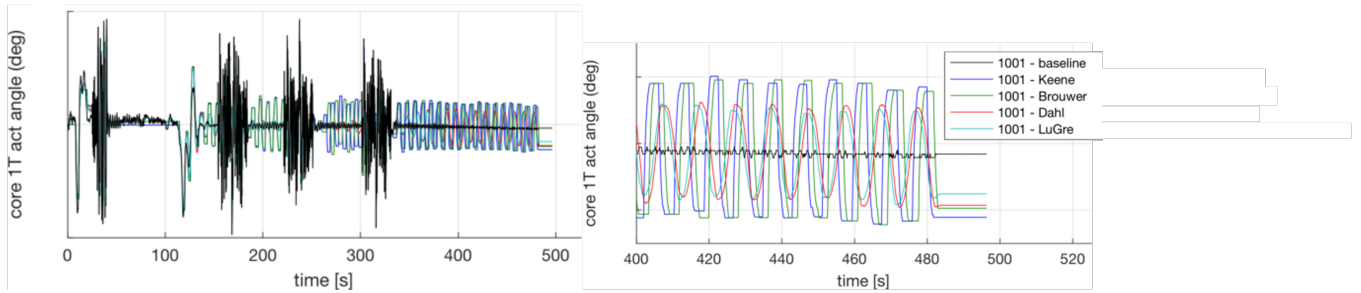
Figure 6. FCS Open Loop Response: Nichols Chart

to Green Run responses and showed the least amplitude dependent effects. The Dahl model was somewhere in between in both respects, exhibiting some amplitude dependence that correlated with the observed response.

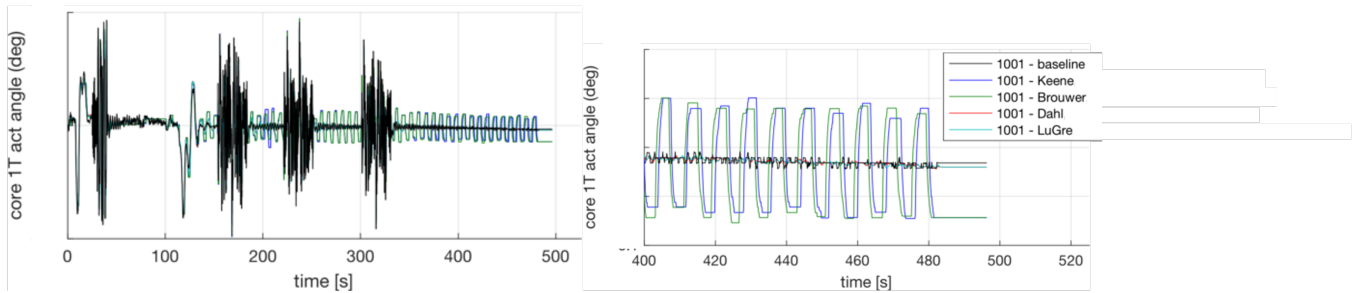
To determine a bound on the possible flight performance, the friction-augmented simplex models were simulated in the Marshall Aerospace Vehicle Representation in C (MAVERIC) 6-DOF time-domain environment under assumptions of either a high or low bounding structural stiffness and friction value. Figure 7 shows an overlay of the yaw engine angle time history responses from a nominal run under the lower stiffness assumption (consistent with the ambient vectoring test data) and at a friction torque of 144,000 in-lbf. The full scale figure on the left shows the onset of a limit cycle oscillation for the friction augmented models following the booster separation event at around 125 seconds. The four areas of high frequency content are the in-flight programmed test inputs (PTIs), a time-scheduled system identification input used for system identification comprised of a multi-sines and sine sweep waveforms. During the PTIs, the limit cycle oscillation does not occur because the larger amplitude of TVC command reduces the extent of the gain and phase degradation. During the quiescent periods at all other flight conditions, the LCO reaches an amplitude of about 0.1 degrees and a frequency between 0.1-0.2 Hz. The right figure shows the detail during the end of the core stage burn, comparing the responses amongst the various friction models. The coulomb models represented by the “Keene” and “Brouwer” lines show a significantly distorted square-wave type response at a higher amplitude where as the Dahl and LuGre models show a smaller amplitude, less distorted, and more sinusoidal response.

Figure 8 shows an overlay of the yaw engine angle time history responses from a nominal run under the higher stiffness assumption (consistent with the hot fire vectoring test data) and at a friction torque of 144,000 in-lbf. As can readily be observed, the increase in stiffness results in no limit cycle oscillation for the Dahl and LuGre models and the magnitude is reduced by half of the previous case for the Coulomb models represented by the “Keene” implementation.

The nominal cases above illustrate that the potential for LCO is dependent the type of friction



**Figure 7. MAVERIC 6-DOF Nominal Response with Bounding Friction Models, Soft Stiffness**



**Figure 8. MAVERIC 6-DOF Nominal Response with Bounding Friction Models: Stiffer Structure**

model, its parameters, and the load stiffness assumptions in the model. To rule out potential interactions with other dynamics in the time domain simulation, selected Monte Carlo simulations were run in with the fiction-augmented TVC simplex models. Figure 9 shows the normalized Flight Control System angle command ratio responses for four different Monte Carlo simulations where the black solid line represents the nominal and is overlaid on the dispersed set of 2000 runs. The upper left plot shows the response of the baseline simulation with no friction effects. The upper left shows the Coulomb implementation with softest stiffness, which demonstrates the highest LCO prediction of the four cases. The bottom two cases are simulated with the Dahl model, showing similar trends to the nominal case where the soft structure (left) shows an LCO and the higher stiffness (right) shows only some evidence of reduced damping for the small amplitudes during quiescent regions. The Monte Carlo simulations demonstrated the same trends as the nominal cases and the dispersed runs did not show evidence of any behaviors not already present in the nominal response.

### 3.3 Frequency Domain Analysis with Softer Structure

Green Run ambient testing revealed that the load stiffness was significantly lower than expected, falling below parameter values used in all prior design and verification analyses. To assess the robustness of the flight control system with respect to this change, flight control system frequency domain analysis was performed with the softer load stiffness parameter. Assessment of high-frequency flex response to this change was of particular interest to the flight control system. In the flight control open loop analysis, core stage global bending modes in the approximately 6+ Hz frequency range exhibit an favorable inertial-servoelastic coupling effect (“tail-wag-dog and dog-wag-tail”) with the TVC system. . Prior to the analysis of the Green Run test data, several key modes in the flight control open loop were assumed to be significantly damped as a result of this effect, yielding benefit to the high frequency gain margins.

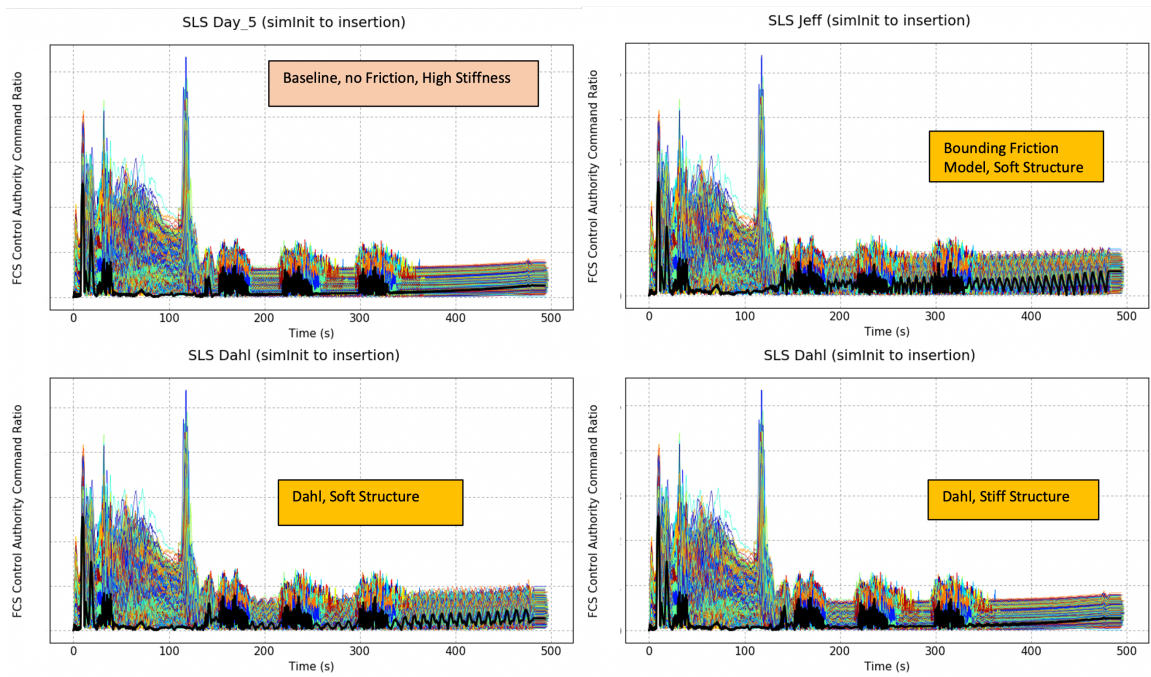


**Figure 9. MAVERIC 6-DOF Monte Carlo Response with Bounding Friction Models**

The flight control open loop frequency-domain analysis showed little sensitivity to the decrease in load stiffness to the observed Green Run ambient test value. Figure 10 (blue: high stiffness, green: low stiffness) shows that high frequency bending attenuation margins were affected by the change of stiffness, but with no determinate trend and, in both cases, margins exceeded the nominal design goal. All other typical stability margins in the flight control system analysis were shown to be negligibly impacted by the change in structural characteristics.

To further investigate the effect of the load stiffness on the structural dynamic response, the flight control team assessed a special loop break in the plant, originally developed to investigate a booster flex-TVC interaction, known as Thrust Vector Servo Elastic (TVSE) resonance.<sup>12</sup> This servoelastic torque response represents an open loop break between the flexible body dynamics and the nozzle inertial coupling (DWT/TWD interface), and provides a means to assess stability closed-loop engines coupled with the vehicle elastic modes. The reduced stiffness increased the gain of some of the response peaks yet the modes generally maintain favorable phasing with respect to the critical point. In all cases, the structural modes are conservatively assumed to have 0.5% viscous damping.

### 3.4 Flight Rationale Acceptance

Given that all prior flight trajectory products were void of the TVC friction effects during SLS design and development, the flight controls team sought to ensure all stakeholder disciplines were properly informed of the potential for LCO so that risk could be assessed. Using the conservative levels predicted by the friction-augmented TVC simplex model results shown in Section 3.2, the SLS Loads and Dynamics team assessed the limit cycle oscillation for impacts and found that the small oscillation was not a concern for flight, particularly as it was only present during quiescent flight conditions and not additive with the PTIs. The remaining key areas that were assessed in-

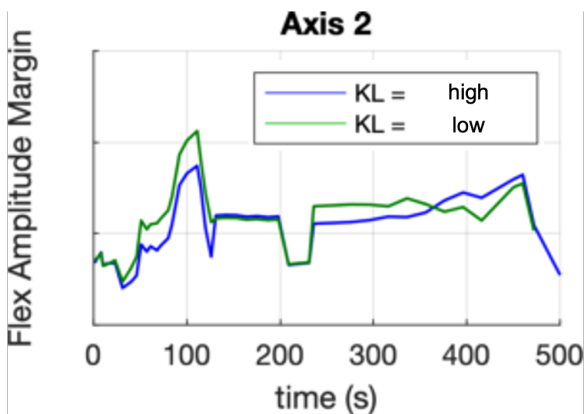


**Figure 10. FCS Flex Stability Margins**

cluded TVC duty cycle impacts on hydraulics, vehicle body rates during separation events, and certification of trajectory-dependent models such as aerodynamics. All disciplines accepted the LCO without concerns. The Day of Launch (DOL) Johnson Space Center mission operations and ground support teams, as well as MSFC backup engineering support teams, were informed of the potential LCO content that might be present on flight displays. With this supporting data and the comprehensive risk evaluation from the relevant disciplines, the step and frequency response requirement deviations were accepted for Artemis I flight based on the acceptability of the friction- and stiffness-driven dynamic effects.

#### **4 FURTHER DEVELOPMENTS FOLLOWING FLIGHT RATIONALE**

Following the acceptance of the bounding predictions, a multi-disciplinary team was formed to further determine the root cause physics and improve the modeling of the friction and stiffness observations seen during the Green Run testing. The simplex model, while a perfectly acceptable means to conservatively predict the effects of amplitude-dependent gain and phase effects of friction, could not fully reproduce the behaviors seen in ambient and hot fire testing. The planar simplex model reduces structural dynamics to the simple spring approximation known as the load stiffness, when in actuality, the structural compliances are distributed on either side of the friction-affected gimbal joint. Furthermore, several revelations about the position and velocity dependence associated with friction itself revealed that advances in the LuGre modeling approach could more accurately represent the amplitude dependent behaviors needed for flight models while maintaining a close match to Green Run results. Companion papers discuss the friction developments and structural dynamics in more detail<sup>2,7</sup> and several key outcomes resulting from the post-wavier assessments are summarized here.

A three dimensional model of the gimbal joint was constructed by the loads team as a FEM with a particular focus on the pitch/yaw degrees of freedom. This FEM of the gimbal by itself was shown to change stiffness based on the load path characteristics in the thrusting versus hanging configuration, providing a partial explanation for the shift observed in load resonance frequency between ambient and hot fire conditions. The FEM was updated for the MASV tool, and a gimbal structural model was provided for each of the two halves (upper and lower parts of the gimbal) and incorporated into the Two Actuator Operational Simulation (TAOS) toolset.

While friction was shown to be negligible in the ambient case, the responses in the Green Run hot

fire conditions clearly necessitated some model of gimbal friction. The MASV simulation approach models the coupling between the structural dynamics and the closed loop actuator system<sup>10</sup> but does not model the gimbal bearing as a separate component; thus, friction effects could not be applied to what was now known as a joint with non-negligible compliance. The Two Actuator Operational Simulation (TAOS) was built for the purpose of modeling 2-axes of simultaneous gimbaling on a single engine with full 3-D mass properties and was the primary simulation used for friction model development after the initial bounding analysis. The TAOS simulation modeled the actuator and load stiffness as in the simplex model but further included the gimbal stiffness DoF of the upper and lower halves to which friction forces could be applied independently.

The TAOS model that incorporated friction forces between the two halves of the gimbal joint provided responses that best matched the Green Run data in step and frequency response. Using an extension of the LuGre model friction that enabled precise tuning of the velocity dependence for vibrational effects, the authors were able to show amplitude dependent effects similar to those observed in the piston responses during Shuttle MPTA.<sup>2</sup>

While the hot fire responses could be well matched by the addition of a thrust-loaded gimbal bearing stiffness coupled with a modified LuGre friction, the change in load stiffness when utilizing the FEM-based unloaded gimbal for ambient condition was not quite low enough to explain the full shift seen in the ambient piston response notch frequencies. The remaining difference was modeled using a decrease in the load stiffness and could produce reasonable matches to frequency response. Figure 11 shows the test comparisons to TAOS model for the ambient (left) and hot fire condition (right) results. In each TAOS case, two gimbal stiffness matrices are included that couple to the engine's six translational and rotational degrees of freedom. Each pair is derived from a FEM that corresponds to the ambient or hot-fire condition, respectively.. Finally, the ambient load stiffness is adjusted (ambient  $K_L = 115,000 \text{ lbf/in}$ , hot fire  $K_L = 205,000 \text{ lbf/in}$ ) to account for the residual mismatch. Modeling and test investigations suggest that amplitude dependent nonlinearities in the unloaded gimbal and/or actuator attach points as well as nonlinear stiffness effects associated with the actuator itself are the cause of the residual differences modeled by the load stiffness change.

Given these exceptional model fits and a nearly complete physics-based rationale for the notch shift between the different conditions at Green Run, the team could more confidently assert that the load resonance in flight boundary conditions is truly higher as reflected in the piston notch transfer function during Green Run hot fire. As was shown during the bounding model analysis, the higher stiffness can reduce the propensity for a limit cycle for a given friction level, especially when the friction effect is modeled using the more physically accurate Dahl/LuGre approaches. This provided some additional evidence to suggest that no LCO would be observed in flight, and plausible explanation for why TVC oscillations were never observed during Shuttle flights. Nonetheless, the bounding model analysis, which used more conservative assumptions, remained a confident rationale for flight even if an oscillation did occur.

While the gimbal stiffness and 2-axis vector friction modeling advancements in TAOS were necessary to reproduce the observed Green Run hot fire response, vehicle time domain simulations for flight rationale employed the linear planar simplex model with adjustments to load stiffness, augmented with a nonlinear friction element. Since the time domain simulation limit cycle potential is driven by the low frequency gain and phase amplitude dependent degradation, the modified LuGre model friction parameters were tuned to produce low frequency amplitude dependence under the assumptions of the simplex model (planar, no gimbal stiffness element) while still maintaining a reasonably good match to the Green Run data. As expected, the simulation results with the stiffer

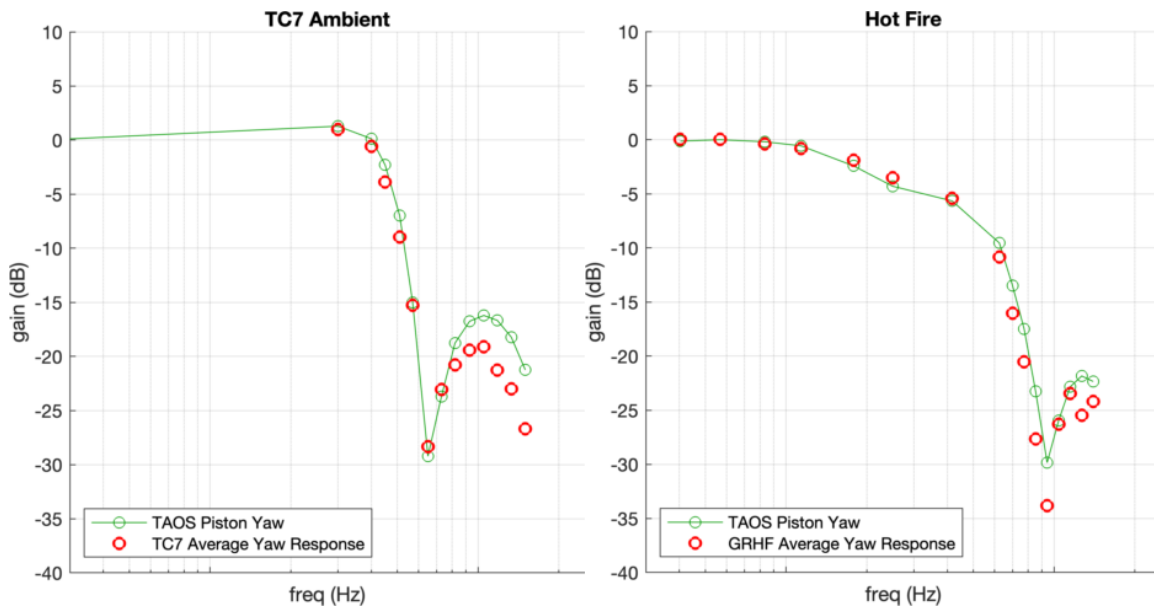


**Figure 11. TAOS Best Fit Modeling vs Test Data: Ambient (Left) and Hot Fire (Right)**

structural stiffness and Green Run-matched LuGre friction parameters did not produce LCO.

## 5 FLIGHT RESPONSES

The SLS Artemis I launch vehicle flew its first and highly successful ascent trajectory on November 16, 2022 with the flight control system performance tracking very close to nominal pre-flight predictions. Figure 12 shows the flight core stage actuator commands in pitch and yaw in comparison to the simulated nominal (day of launch winds incorporated) and statistical bounds derived from Monte Carlo simulations. While the nominal simulation case here contains prediction of friction that does not produce an LCO, the core flight responses not during the PTIs show some small amplitude-persistent frequency content, with a period of oscillation consistent with a friction-induced limit cycle.

### 5.1 Preliminary Post Flight Evaluation

Given the presence of a time response in quiescent flight that suggested gimbal friction effects, the SLS flight control team assessed in-flight system identification data to evaluate whether friction could be observed in the flight control loop. The responses derived from the targeted excitations produced by the Programmed Test Inputs (PTI) were found to produce some of the most significant supporting data. The in-flight PTI approach, based on a carefully scheduled and optimized input command profile, was previously demonstrated on the Ares I-X flight test<sup>13</sup> and supports in-flight model validation using small-amplitude TVC actuator commands. The PTI maneuvers are comprised of multi-sine and sine sweep waveforms of commands near the flight control-observable frequencies to enable the open loop flight control response and associated vehicle loop stability margins to be reconstructed from telemetered flight data during otherwise quiescent flight times. Also enabled by the small amplitude PTI was the ability to reconstruct the frequency response between the actuator commands and telemetered piston position response.

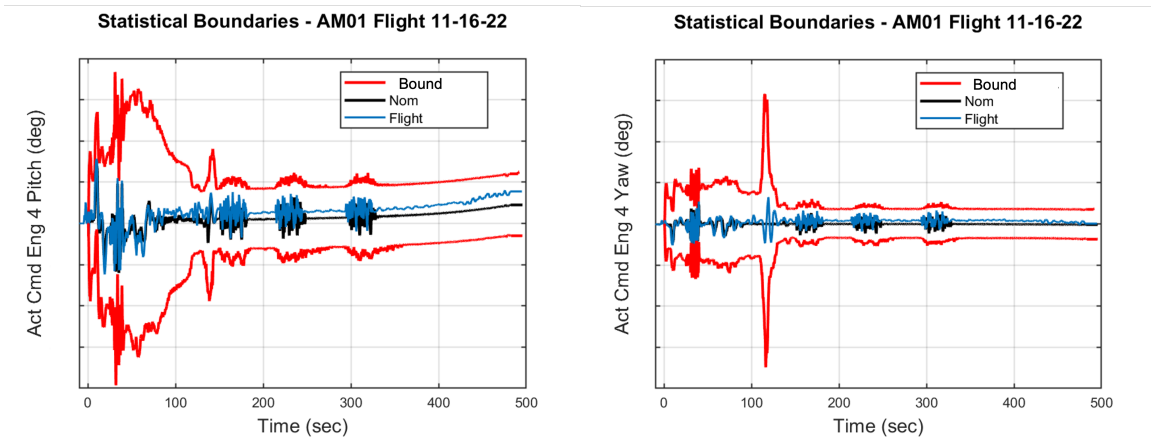


**Figure 12. Artemis I Flight vs Predicted: Core Engine Actuator Commands**

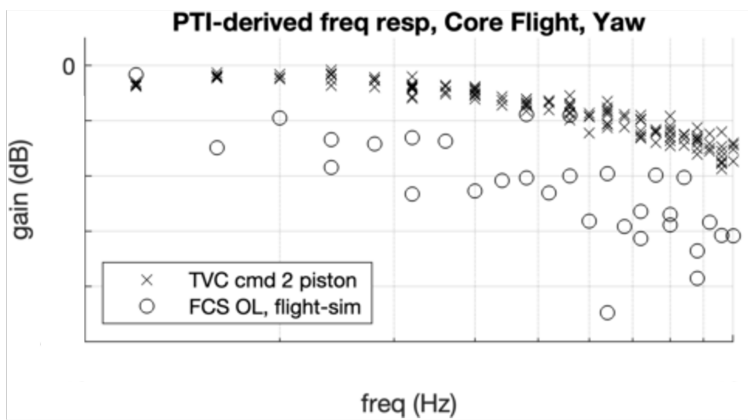


**Figure 13. Artemis I Flight Frequency and Time Response during PTI**

Figure 13 shows yaw frequency responses derived from the PTI during core stage of flight using the three multi-sine waveforms. The TVC commands to piston data (“TVC cmd 2 piston”) shows a similar gain degradation as observed during the Green Run testing. whereas the difference between the FCS open loop and flight simulation (“FCS OL, flight-sim”) produces even lower gain at low frequency. While the piston reflects only the actuator’s response to commands, the FCS open loop necessarily involves the engine angle response and its lower observed gain would be consistent with friction effects, as discussed in Section 3.1. Although a direct measurement of engine position was not available in flight, the open-loop flight control response as derived from the PTI maneuver necessarily results from some gain reduction in the forward path and would reflect any changes in the engine response gain with respect to commands. Since the PTI command magnitudes at the core phase flight times range are smaller than the Green Run amplitudes, the observed gain reduction in the FCS open loop is consistent with a friction-influenced engine response.

Aside from the fact that the higher Green Run amplitudes and limitations of the string pot engine measurement made firm quantification of friction difficult, initial observations suggest that the flight friction environment was slightly higher than that observed in Green Run. Three plausible explanations have been considered. First, the two-axis simulations with the Green Run-tuned friction model

in TAOS showed that during Green Run commanding, the higher frequency commanded motion orthogonal (on the opposing TVC axis) to the lower frequencies appeared to produce a dither effect, thereby reducing the influence of friction observed in the low-frequency axis. Except during the intentional commanding during the PTI periods, no such higher frequency content was visible in the flight data. Secondly, a comparison of apparent noise levels on the piston measurements between Green Run and flight showed that flight environments were significantly less severe than during the sea level hot fire testing at the Stennis Space Center (SSC) B2 stand, as expected due to a lack of reflected acoustics. This suggests that friction levels may have been lower at Green Run than in flight due to the more severe environments in the test condition. Lastly, the Green Run thrust level was necessarily lower than in flight since the engines are operated at sea level. While this scale factor (and the mass of the engines) was accounted for in the flight predictive models, potential nonlinear dependence on thrust magnitude was not modeled since the Green Run TVC vectoring was performed at a single thrust level.

## **5.2 Outlook for Future Flights**

The revelations occurring throughout the course of SLS Green Run TVC test efforts, associated post-test analysis, and ultimately, successful flight have significantly advanced the confidence of NASA's flight controls discipline in predicting and assessing performance of the Core Stage TVC system. The culmination of evidence afforded by advanced friction modeling techniques and confident determination of the load stiffness in hot firing conditions supports the conclusion that friction effects can be expected, yet remain at the small, acceptable levels as bounded by the Artemis I pre-flight predictions. The SLS flight control and TVC teams will continue their focus on an advanced TVC modeling approach specific to each vehicle, with special emphasis on the evolution to the heavier Block 1B vehicle, currently scheduled as the fourth flight of SLS.

## **6 CONCLUSIONS**

In the development of launch vehicle thrust vector control systems, comprehensive test-based evaluation of the TVC performance in flight-like boundary conditions will always uncover unexpected or unmodeled physical phenomena. Hot-fire frequency and transient response testing to elucidate friction parameters and determine the fully-coupled load resonance characteristics is essential in any development program. The SLS Program's findings during multiple TVC tests, advances in friction and structural modeling, analysis of the underlying physics, and ultimately the first flight of Artemis I challenged longstanding assumptions and modeling approaches regarding friction in the Core Stage TVC system. Through these experiences, the SLS flight control and TVC teams have improved the state of the art in modeling the complex interplay of friction and structure. This foundation of data and experience will help reduce cost, minimize risk, and maximize mission capability as NASA shapes the SLS generation of heavy-lift launch vehicles.

## **ACKNOWLEDGMENTS**

The authors would like to thank several key persons who made significant contributions in support of this work: Jeff Brouwer developed a simple method for numerical implementation of Coulomb friction, and provided unwavering support for all aspects of this work. The authors are grateful to Charlie Hall for his long term support of the SLS flight controls team and the activities surrounding Green Run and flight; Ivan Bertaska for his leadership of the SLS Ascent Controls Working Group; and Jimmy Compton, Young Kim, and Jason Bush for their support of the flight controls team and

GN&C/Vehicle Management discipline in pursuit of comprehensive testing and analysis of the SLS Core Stage TVC system. This work was supported by the NASA Marshall Space Flight Center under contract number 80MSFC18C0011.

## REFERENCES

- [1] Wall, J., Russell, C., Moore, R., Orr, J., Alaniz, A., Ryan, S., “Design, Instrumentation, and Data Analysis for the SLS Core Stage Green Run Test Series,” AAS-23-152 ,American Astronautical Society GN&C Conference, Feb 2-8, 2023.
- [2] Russell, C., Brouwer, J., Ryan, S., and Stepp, N. “Gimbal Bearing Friction in the Core Stage TVC System,” AAS 23-154, American Astronautical Society GN&C Conference, Feb 2-8, 2023.
- [3] Brouwer, J., “Notes on the Titan IV Coulomb Friction Modelling Approach,” DRAFT 2, Troy 7, Inc. January 31, 2022
- [4] Barrows, T., “Keene Model of Coulomb Friction,” Draper Memo, April 24, 2017
- [5] Dahl, P. R., “A Solid Friction Model,” Space and Missile Systems Organization, TR-77-131, 1977.
- [6] Olsson, H., Åström K.J., Canudas de Wit, C., Gäfvert, M., and Lischinsky, P., “Friction Models and Friction Compensation,” *European Journal of Control*, vol. 4, no. 3, pp. 176-195, 1997.
- [7] Moore, R. et al. “Structural Dynamics Observations in Space Launch System Green Run Hot Fire Testing,” AAS 23-156, American Astronautical Society GN&C Conference, Feb 2-8, 2023.
- [8] McDermott, et al., “Space Shuttle Ascent Flight Control Actuation Subsystem Data Book,” SSD93D0595, Rockwell, September, 1993.
- [9] Gerstner, B. A., “MPT Engineering Analysis Second Interim Report Static Firings S/F-5A Through S/F-12” Rockwell Report STS 81-0254, May 1981.
- [10] Orr J., et al., “Advanced Modeling of Control-Structure Interaction in Thrust Vector Control Systems,” AAS 23-157, American Astronautical Society GN&C Conference, Feb 2-8, 2023.
- [11] Thompson Z., “A Mathematical Model for a Space Vehicle Thrust Vector Control System,” MS Thesis, University of Tennessee, NASA Report 67-34613, Aug 24, 1967.
- [12] Orr, J., Wall, J., and Barrows, T., “Simulation-Based Analysis and Prediction of Thrust Vector Servoelastic Coupling,” AAS 20-091, American Astronautical Society Guidance, Navigation, and Control Conference, 2020.
- [13] Brandon, J. et al, “Ares-I-X Stability and Control Flight Test: Analysis and Plans” AIAA Space Conference and Exposition, San Diego, CA, September 9, 2008.
- [14] Stuart, B., et al., “Overview of the SLS Core Stage Thrust Vector Control System Design,” AAS 23-152, American Astronautical Society Guidance, Navigation, and Control Conference, February 2023.
- [15] Orr, et al., “Advanced Modeling of Control-Structure Interaction in Thrust Vector Control Systems,” AAS 23-153, American Astronautical Society Guidance, Navigation, and Control Conference, February 2023.
- [16] Stuart, B., et al., “Core Stage TVC Systems Engineering Challenges in Reusing Heritage Hardware,” AAS 23-154, American Astronautical Society Guidance, Navigation, and Control Conference, February 2023.
- [17] NASA Engineering Safety Center Technical Bulletin No. 22-05: Launch Vehicle Flight Control Stability Margin Reduction Considerations, August 1, 2022